# Performance Analysis of Different Loaded and Unloaded Wire Antennas as EMI Sensors

S. Ghosh  and  A. Chakrabarty

*Indian Institute of Technology, Kharagpur-721 302*

## ABSTRACT

This paper presents with the performance of different loaded (e.g. inverted L, T, I and C-shaped antennas) and unloaded wire antennas as electromagnetic interference (EMI) sensors. To determine electromagnetic radiation from an electronic component, it is required to evaluate the field strength at a certain distance from it using the sensor. The most common performance descriptor of a sensor is its antenna factor. Here, the method of moments with pulse basis function and point-matching technique has been used to evaluate the current distribution on the antenna surface, and hence, the antenna factor of different wire antennas. The same theory for unloaded antennas has been extended for different loaded-wire antennas. The loaded antennas in transmitting mode are widely used for low-frequency communication. However, while using these antennas as EMI sensors, the extra loading is likely to introduce the reception of cross-polarised component of incident electric field. This paper highlights the results of the initial investigation on the performance of these loaded antennas as EMI sensors in terms of the antenna factor for the desired and cross-polarised component of incident electric field.

**Keywords:** Wire antenna, loaded wire antenna, EMI sensor, antenna factor, method of moments

## 1. INTRODUCTION

The increased use of electronic equipment in modern day technologies causes electromagnetic interference (EMI) with each other. To avoid this interference episode different regulatory committees in different countries have set some standards of electromagnetic emission. All the electronic devices must conform to these standards. By measuring the radiated electric field due to that equipment, the compliance of the devices conforming to the standards of interference is tested. The measurement is performed inside an anechoic chamber, GTEM Cell, shielded chamber or in open area test site (OATS) which are made free from other electromagnetic

radiation by putting the receiver at a specific distance from the device under test. The EMI sensors in common use are dipoles or loop antennas (e.g., Anritsu dipole MP651A/B). Wire antennas are widely used as transmitting antenna and as sensor for EMI measurements. The term wire refers to metallic, highly conducting wire or wire-like structures. For EMI measurement, it is required to determine the field strength at the point of measurement using the sensor. To use these sensors for this purpose, a calibration data is required relating the electric field at the aperture of the receiving antenna to the voltage at the 50 Ω matched detector. The ratio of incident electric field at the surface of the

sensor to the received voltage at the antenna terminal is known as the antenna factor[1]. So for EMI measurements, it is of utmost importance to know the antenna factor of the sensor at the frequency of measurement. This calibration can be performed experimentally by rigorous, time consuming and expensive measurements. Here, a theoretical method based on numerical technique of method of moments has been evolved to predict the antenna factor of different wire antennas. The computer-aided evaluation is a better one than the experimental one since it reduces the measurement hazards and also it considers the variety of sensors much easily than the experimental one.

The theoretical studies of different types of transmitting and receiving wire antennas have interested numerous researchers for decades[2-8]. At low frequencies, the electrical length of the antenna to achieve self-resonance becomes very large. For this case, proper loading of the antenna is employed to reduce the resonant length of the antenna. The loaded antennas (e.g., inverted L, T, I and C-shaped antennas) are widely used for low frequency communication[2]. Also, the broadband performance of a dipole loaded with circular disc had been studied as EMI sensor[3]. However, the extra loading is likely to introduce the reception of cross-polarised component of incident electric field that may degrade the performance of the sensor. Hence, while using these loaded systems as sensors, the cross-polarisation characteristics must be known. In this study, the authors concentrated on the characterisation of the loaded antennas as EMI sensors in terms of the antenna factor for the desired and cross-polarised incident electric field. The results have been compared with the data available in literature, wherever possible[3].

## 2. ANALYSIS

### 2.1 Boundary Condition

The geometry of the conducting wire is shown in Fig. 1(a). An incident electric field of 1V/m is considered which impinges on the surface of a perfectly conducting wire. The following assumptions are made to simplify the analysis:

- The wire is perfectly conducting.

- The wire radius is taken to be much less than the wavelength, it can be assumed that only $z$-directed currents are present.

In general, the incident unit plane wave at the scatterer is expressed as follows:

$$E^i = u_t e^{-jk_t \cdot r_n} \qquad (1)$$

For simplification of the problem, it is considered that the incident wave is coming from $\theta_i = \dfrac{\pi}{2}$

This incident field induces a linear current density $J_s$ which reradiates and produces an electric field that is referred as the scattered electric field $E^s$. The other field present[4] is the incident field $E^i$.

$$E^t(r) = E^i(r) + E^s(r) \qquad (2)$$

At the surface of the $z$-directed wire and also interior to the wire, the sum of the $z$-directed scattered field and the $z$-directed incident field must be zero.

i.e.

$$E_z^t(r = r_s) = E_z^i(r = r_s) + E_z^s(r = rs) = 0 \qquad (3)$$

The scattered electric field for the situation in Fig.1 is given as

$$E^s = -j\omega\mu A - \nabla\phi \qquad (4)$$

where A is the magnetic vector potential and $\phi$ is the scalar potential.

Considering the wire radius to be much less compared to the wavelength, Eqn (4) is simplified as follows:

$$E_z^s(r) = \frac{-j}{\omega\mu\varepsilon}\left[k^2 A_z + \frac{\partial^2 A_z}{\partial z^2}\right] \qquad (5)$$

Neglecting the edge effects, the $z$-component of $A$ is expressed as

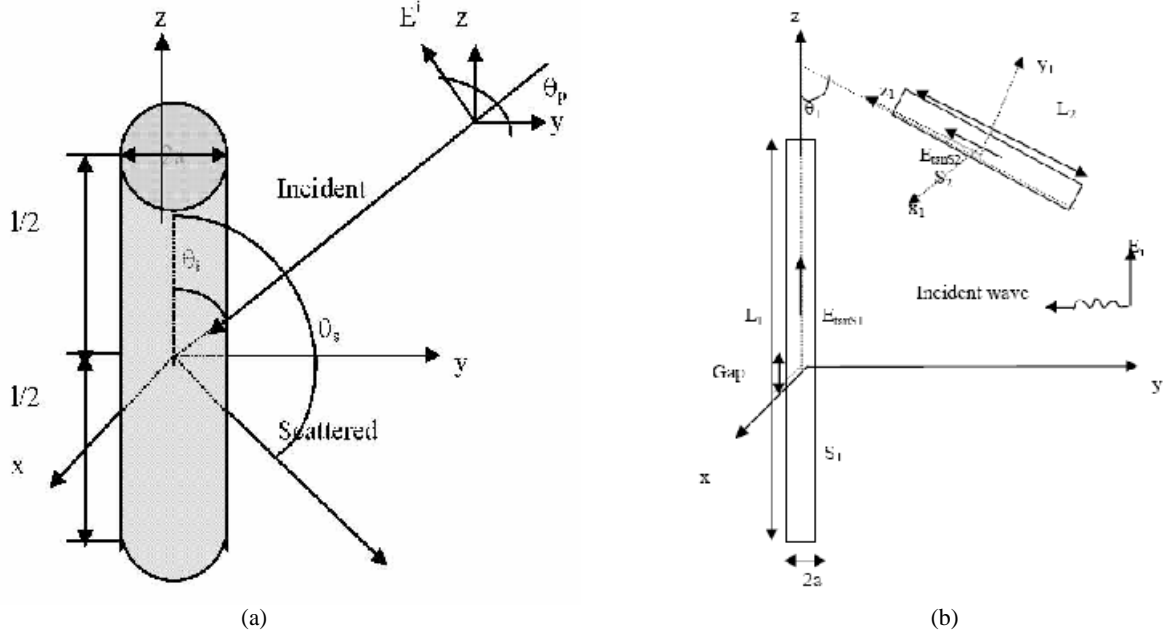$$A_z = \frac{\mu}{4\pi}\iint J_z \frac{e^{-jkR}}{R} ds' \qquad (6)$$

**Figure 1. (a) Plane wave incidence on a wire antenna, and (b) wire antenna with parasitic element.**

Here, $R$ is the distance between the source point $(x',y',z')$ and observation point $(x,y,z)$, i.e.,

$$R = \sqrt{(x-x')^2 + (y-y')^2 + (z-z')^2}$$

$$= \sqrt{\rho^2 + a^2 - 2\rho a \cos(\phi - \phi') + (z-z')^2}$$

Considering the wire as very thin, the current density (independent of the azimuthal angle $\phi$) is expressed in terms of $I_z(z)$, i.e., the equivalent line-source current located on the surface of the wire. For observations on the surface, Eqn (5) reduces as follows:

$$A_z(\rho = a) = \mu \int_{-l/2}^{l/2} I_z(z')G(z,z')dz' \qquad (7)$$

Here, $G(z,z') = \dfrac{1}{2\pi}\int_0^{2\pi} \dfrac{e^{-jkR}}{4\pi R}d\phi'$ and

$$R(\rho = a) = \sqrt{4a^2 \sin^2(\frac{\phi'}{2}) + (z-z')^2}$$

For very thin wire, $(a<<\lambda)$

$$G(z,z') = G(R) = \frac{e^{-jkR}}{4\pi R}$$

Applying Eqns (5)-(7), Eqn (3) is simplified as

$$\int_{-l/2}^{l/2} I_z(z')\frac{e^{-jkR}}{4\pi R^5}\left[\begin{array}{l}(1+jkR)(2R^2-3a^2)\\ +(kaR)^2\end{array}\right]dz'$$

$$= -j\omega\varepsilon E_z^i(\rho = a)$$

(8)

For more general case, i.e., for the incident field in $\theta_i \neq \dfrac{\pi}{2}$ direction, a relative phase of $\exp(j\beta(n-1)\Delta l_n \cos\theta_i)$ is introduced at different points on the surface of the wire.

*2.1.1 Loaded Antennas*

A wire antenna was considered with an inclined arm making an angle $\theta_l$ with the axis of the antenna element (Fig. 1(b)). To simplify the problem first the inclined arm was considered to be placed in the y-z plane with $x = 0$. An incident z-directed electric field of 1V/m impinges on the surface of

335

a perfectly conducting wire. As before the boundary condition $E_{\tan}^{total} = 0$ over the conducting wire was applied.

The surface of the antenna is defined as $S_1$ and that of the other element as $S_2$. The total electric field contains the components of incident electric field $E^i$ and scattered electric field $E^s$. The total tangential fields on $S_1$ and $S_2$ are written as follows:

$$E_{\tan_{S_1}} = E_{S_1}^i + E^S{}_{\tan_{S_1,S_1}} + E^S{}_{\tan_{S_1,S_2}} = 0 \qquad (9a)$$

$$E_{\tan_{S_2}} = E_{S_2}^i + E^S{}_{\tan_{S_2,S_1}} + E^S{}_{\tan_{S_2,S_2}} = 0 \qquad (9b)$$

where terms $E_{\tan_{S_1}}$, $E_{\tan_{S_2}}$ in Eqn (9) are the total tangential electric field on $S_1$ and $S_2$ respectively; $E_{S_1}^i$, $E_{S_2}^i$ are the incident electric field on $S_1$ and $S_2$ respectively; $E^S{}_{\tan_{S_1,S_1}}$, $E^S{}_{\tan_{S_1,S_2}}$ are the angential component of scattered electric field on $S_1$ due to current distribution on $S_1$ and $S_2$ respectively; and $E^S{}_{\tan_{S_2,S_1}}$, $E^S{}_{\tan_{S_2,S_2}}$ are the tangential component of scattered electric field on $S_2$ due to source on $S_1$ and $S_2$ respectively.

The related field components are evaluated considering thin wire approximation.

To evaluate the scattered electric field due to the parasitic element, it was found convenient to define a new rectangular coordinate system $(x_1, y_1, z_1)$ with its origin at the origin of the element and its $z$-axis parallel to the axis of that element [Fig. 1(b)].

Applying the boundary condition on the wire elements, the $z$-directed electric field components for Eqn. 9(a) are written as follows:

$$E_{S_1}^i = E_z^i \; ;$$
$$E^S{}_{\tan_{S_1,S_1}} = E^S{}_{z_{S_1,S_1}}$$
$$E^S{}_{\tan_{S_1,S_2}} = E^S_{z_1 S_1,S_2} \cos\theta_1 + E^S_{y_1 S_1,S_2} \sin\theta_1 \qquad (10)$$

The field components $E^S_{z_{S_1,S_1}}$, $E^S_{z_1 S_1,S_2}$ are the z-components of scattered electric field on $S_1$ due to current distribution on $S_1$ and $S_2$ respectively;

$E^S_{y_1 S_1,S_2}$ is y component of scattered electric field on $S_1$ due to current distribution on $S_2$; and $\theta_1$ is the angle of inclination of the parasitic element with the axis of the main arm.

For Eqn. 9(b), the field components are as follows:

$$E_{S_2}^i = E_z^i \cos\theta_1 \; ;$$
$$E_{\tan_{S_2,S_1}} = E^S{}_{z_{S_2,S_1}} \cos\theta_1 - E^S{}_{y_{S_2,S_1}} \sin\theta_1 \qquad (11)$$
$$E_{\tan_{S_2,S_2}} = E^S{}_{z_1 S_2,S_2}$$

where, $E^S_{z_{S_2,S_1}}$, $E^S_{z_1 S_2,S_2}$ are the z-component of scattered electric field on $S_2$ due to current distribution on $S_1$ and $S_2$ respectively and $E^S_{y S_2,S_1}$ is the y component of scattered electric field on $S_2$ due to current distribution on $S_1$.

The same technique can be extended for different loaded antennas with the parasitic element/elements in electrical contact to the main arm (e.g., inverted L, T, I, C antennas, broadband dipole, i.e., a dipole loaded with circular disc) (Fig. 2). Each circular disc of the broadband dipole is replaced by a large number of wires placed in the x-y plane and perpendicular to $z$-axis. To enforce the boundary condition on the surface of each element, the expressions for the tangential component of the electric field on each element have been evaluated in terms of the corresponding $x$, $y$, $z$ components of scattered and incident electric field.

For a wire structure with interconnected wires, the continuity equations are to be satisfied at the element interconnections[8]. For two wires connected with their second ends, the continuity equation for the interconnecting node is written in the form

$$I^{(1)} (s = L) + I^{(2)}(s = L) = 0 \qquad (12)$$

where $I^{(1)}(s)$ and $I^{(2)}(s)$ are the total currents along the first and second wire respectively.

The expressions for the scattered electric field are available in the literature[9] and hence, not repeated here. Putting the simplified expression for the scattered
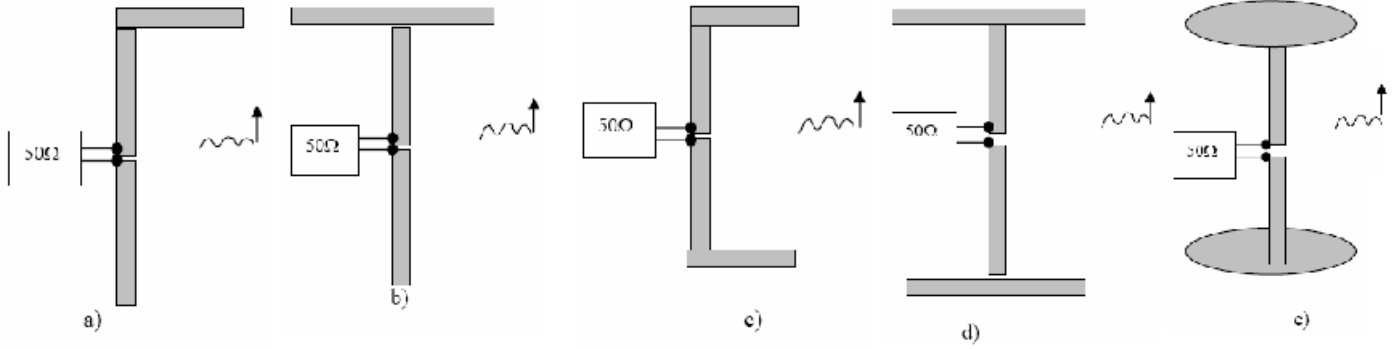
**Figure 2. (a) Inverted L-shaped sensor, (b) T-shaped sensor, (c) C-shaped sensor, (d) I-shaped sensor, and (e) broadband dipole.**

electric field, Eqn (9) have been transformed to an integral equation involving the unknowns used to describe the current distribution on the surface of the wire and the known incident electric field on the other side of the equation.

## 2.2 Matrix Solution

Here the method of moments with pulse expansion function and point-matching technique has been used[10]. A simple solution to Eqn (8) is obtained by approximating the integral as the sum of integrals over $N$ small segments. The current density is considered as constant throughout a particular segment. These $N$ segments can be considered as an $N$-port network, and the wire object is obtained by short-circuiting all ports of the network. Hence, by defining the current matrix as

$$[I] = \begin{bmatrix} I(1) \\ I(1) \\ . \\ . \\ I(N) \end{bmatrix}$$

and the voltage excitation matrix as

$$\left[ V^i \right] = \begin{bmatrix} E^i(1).\Delta l_1 \\ E^i(2).\Delta l_2 \\ . \\ E^i(N).\Delta l_N \end{bmatrix} \qquad (13)$$

Equation (8) is rewritten as

$$[V^i] = [Z][I] \qquad (14)$$

From Eqn (14), the current distribution on the wire is found by solving simple matrix equation.

## 2.3 Antenna Factor

The ratio of the incident electric field on the surface of the sensor to the received voltage at the antenna terminal when terminated by 50 Ω load is known as Antenna Factor[1].

$$\text{Antenna Factor} = \frac{\text{Incident electric field } (E^i)}{\text{Received voltage } (V)} \qquad (15)$$

The Thevenin's equivalent circuit diagram of an EMI sensor is shown in Fig. 3. The receiving antenna is replaced by an equivalent open circuit voltage at the two terminals of the antenna and its impedance. Generally the receiver (e.g., spectrum analyser) impedance is considered as 50 Ω. The open circuit voltage $V_{oc}$ at the gap of the antenna is related to the incident electric field on the antenna surface. The incident electric field $E^i$ over each point on the wire antenna is uniform, whereas the impressed currents so produced on the wire are non-uniform. So to make an average, a crude approximation is made by introducing the effective length of the antenna, which when multiplied by the feeder current $I_{sc}$, equals to the integration of the impressed current over the length of the wire. Accordingly, the effective length is written as
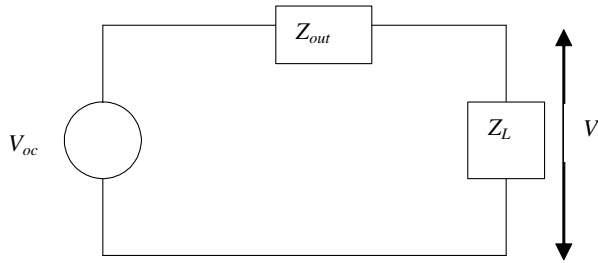
337

**Figure 3. Equivalent circuit diagram of a sensor.**

$$l_{effective} = \frac{\int_{-l/2}^{l/2} I.dl}{I_{sc}} \qquad (16)$$

The open circuit voltage, $V_{oc}$ at the end terminals is written as

$$V_{oc} = \vec{E}_i.\vec{l}_{effective} \qquad (17)$$

The integral in Eqn (16) is approximated by the summation over $N$ subsections as

$$l_{effective} = \frac{\sum_{n=1}^{N} I_n.\Delta_n}{I_{sc}} \qquad (18)$$

The output impedance of the antenna is written as

$$Z_{out} = \frac{V_{oc}}{I_{sc}} \qquad (19)$$

From the equivalent circuit diagram, the voltage to the receiver is achieved as follows:

$$V = \frac{Z_L}{Z_L + Z_{out}} V_{oc} \qquad (20)$$

Generally, $Z_L$ i.e., impedance of the detector (e.g., spectrum analyser) is considered as 50 Ω.

To avoid the inaccuracy due to the approximations made in the evaluation of the open-circuited voltage in terms of the effective length of the antenna, the concept of the concentrated load is used later[8]. In this method the load connected with the antenna is considered to be concentrated within the gap of the sensor. Hence, Eqn (14) is modified as

$$[V^i]=[Z'\ ][I] \text{ with } [Z']=[Z]+[Z_C] \qquad (21)$$

where $[Z_C]$ is a diagonal matrix with only one non-zero diagonal element.

Solving Eqn (21) following the same method, will give the current through the load, which when multiplied by the load will directly give the output voltage.

## 2.4 Cross-polarisation Effect

Due to the presence of the top and bottom loading, loaded sensors (Figs 2 (a) to 2 (d)) are likely to suffer from cross-polarisation pick-up. Hence while dealing with loaded antennas, the cross-polarisation characteristics of the antennas should be known. Here, these studies have been performed in terms of the antenna factor of these antennas for the desired and cross-polarised electric field [Figs 4 (a) and 4 (b)].

## 3. RESULTS

This study deals with the evaluation of antenna factor of different loaded and unloaded wire antennas. The antenna factor versus L/λ graph for a wire antenna is shown in Fig. 5. Also the antenna factor data supplied by the manufacturer for an Anritsu dipole (MP651A) antenna has been compared with the theoretical antenna factor (Fig. 6).

Investigations have been extended for loaded wire antennas. Figures 7 and 8 show the load arm lengths for various main arm lengths to obtain the resonant effect and corresponding resonance resistance of inverted L, T, I, and C-antenna. The results are obtained as the output of huge computation time and efforts. These data for the main arm length and the corresponding load arm length to achieve resonance in the transmitting mode have been used to study the antenna factor of these antennas in the receiving mode. The antenna factor of different loaded sensors for the desired and also for the cross-polarised incident electric field is shown in Figs 9 to 12. The theory has been verified with the experimental result (Fig. 13) for the broadband dipole available in literature[7]. The dimension of different parts of the antenna are given below:
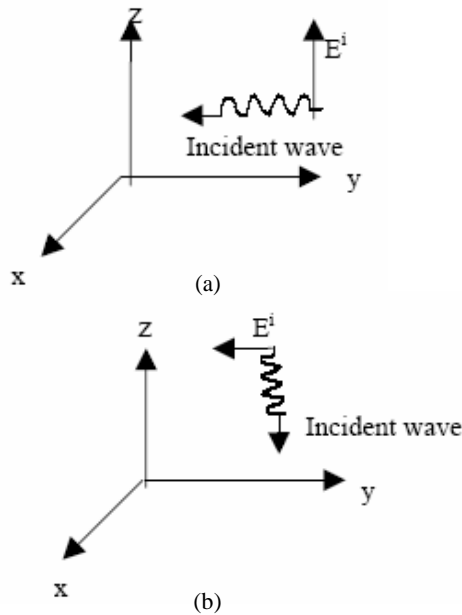
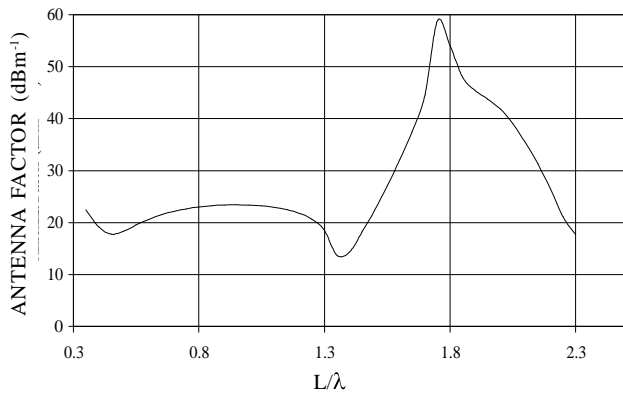Figure 4. (a) Desired polarisation of incident field; (b) Cross-polarisation of incident field.

- Length of the central part of broadband dipole antenna = 0.54 m

- Radius of the central part of the dipole = 2.244 cm

- Radius of the capacitive hats = 8.9 cm

- Number of wires used to represent each circular disc = 12

## 4. DISCUSSIONS

In this study, extensive analysis has been performed on different loaded and unloaded wire antennas in receiving mode as EMI sensors. Though the theory applied is the extension of the classical theory, a genuine effort has been made to make a case



Figure 5. Antenna factor versus L/λ with radius=0.004 λ.
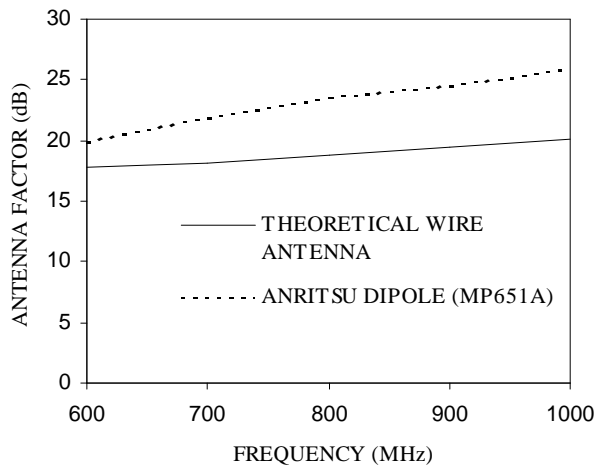


Figure 6. Comparison of antenna factor of theoretical wire antenna with the Anritsu dipole MP651A antenna.
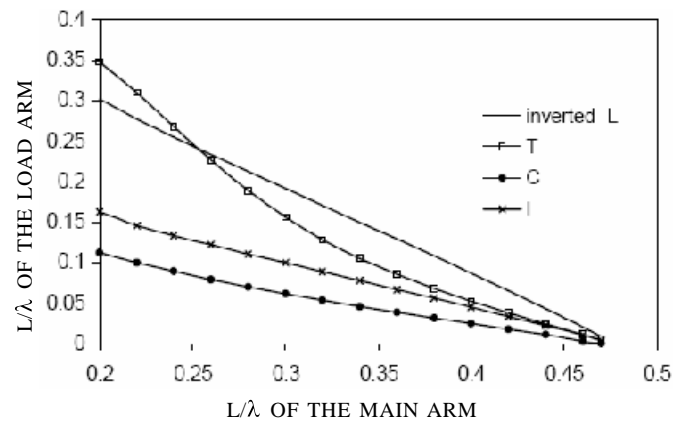


Figure 7. Length in λ of the load arm versus corresponding length in λ of the main arm of loaded antennas.
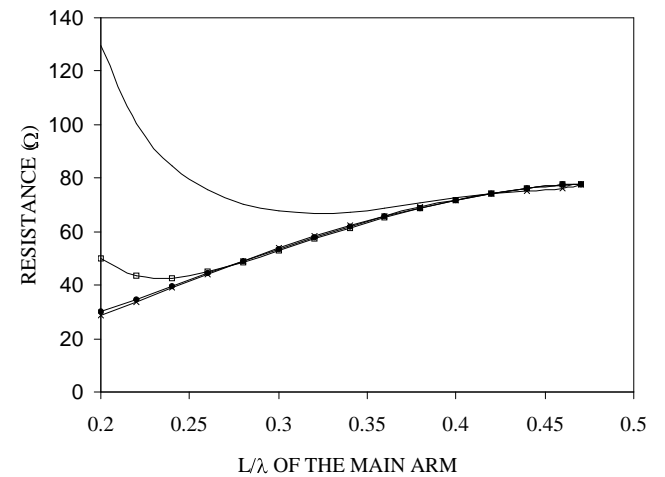


Figure 8. Resonance resistance versus corresponding length of the main arm of loaded antennas.

study of different loaded configurations to get lower value of antenna factor in a frequency band and sometimes at the cost of cross-polarisation effect.

An antenna with lesser antenna factor behaves as a better receiver. From the plot of antenna factor versus $L/\lambda$ (Fig. 5) it is seen that the antenna acts as a good receiver when its length is between $0.35\lambda$ to $1.35\lambda$. The theoretical value of antenna factor had been compared with the chart supplied by the manufacturer of an Anritsu Dipole MP651A. The length of the Anritsu dipole arms and the diameter had been measured for different frequencies. The same values of length and diameter were

incorporated in the software programs for numerical evaluation of antenna factor.

From the graph of frequency versus antenna factor for the two cases (Fig. 6) it is seen that the theoretical value of antenna factor is less, i.e., the theoretical antenna acts as a better receiver compared to the supplied one. It seems that the presence of the balun circuitry and insulating covering material had increased the complexity of the Anritsu dipole that causes the degradation of its performance as a good receiver.

The same method with suitable boundary condition is extended for loaded wire antennas (e.g., inverted L, T, I, and C-antennas).

Studies show that the antenna factor for the desired polarisation for all these reduced height sensors did not show significant change from the corresponding antenna factor of unloaded dipole of resonant length (which is usually higher in length than the loaded length). The advantage has been achieved in terms of the reduction of main arm length. From the study of the cross-polarisation pick-up and cross-polarisation isolation, the following points are noticed:

- The plot of antenna factor of the inverted L-shaped antenna (Fig. 9) shows a cross-polarisation isolation of better than 0.8 dBm$^{-1}$.

- The cross-polarisation isolation for T-shaped antenna (Fig. 10) is better than 73.4 dBm$^{-1}$.
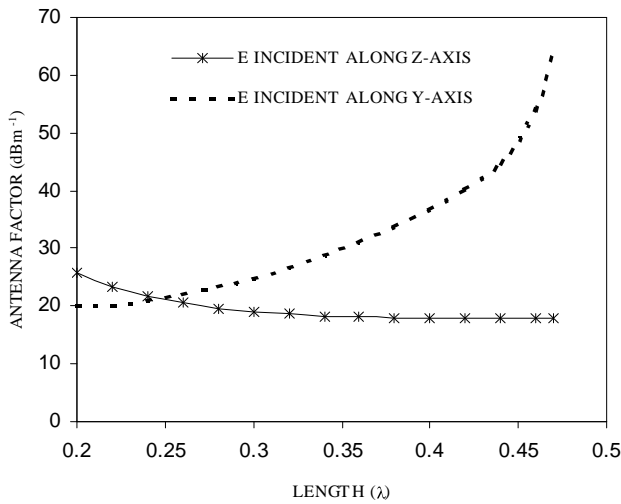


**Figure 9. Antenna factor versus resonant length of inverted L-shaped antenna.**
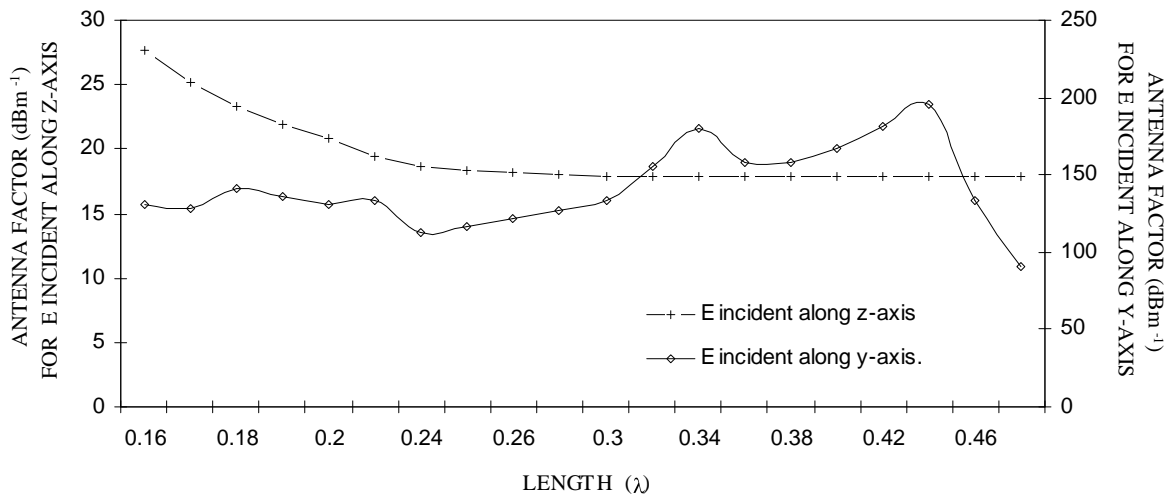


**Figure 10. Antenna factor versus length in wavelengths of T-shaped antenna.**
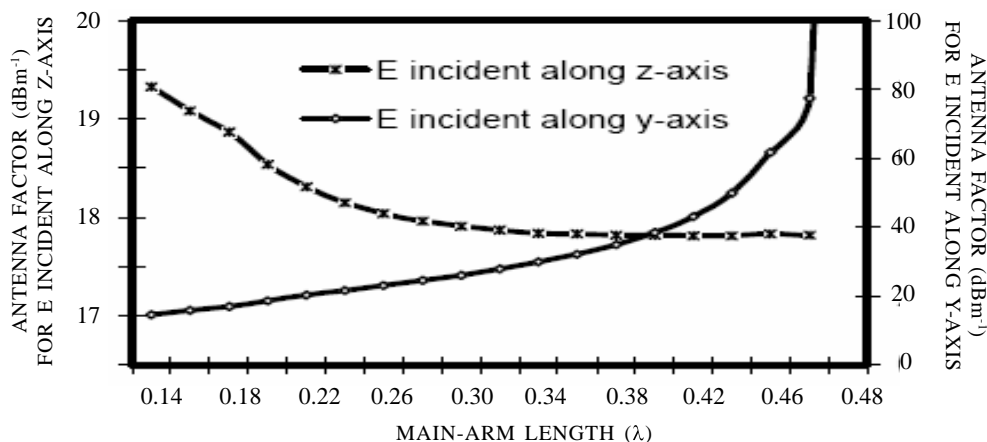
**Figure 11. Antenna factor versus length in wavelengths of C-shaped antenna.**
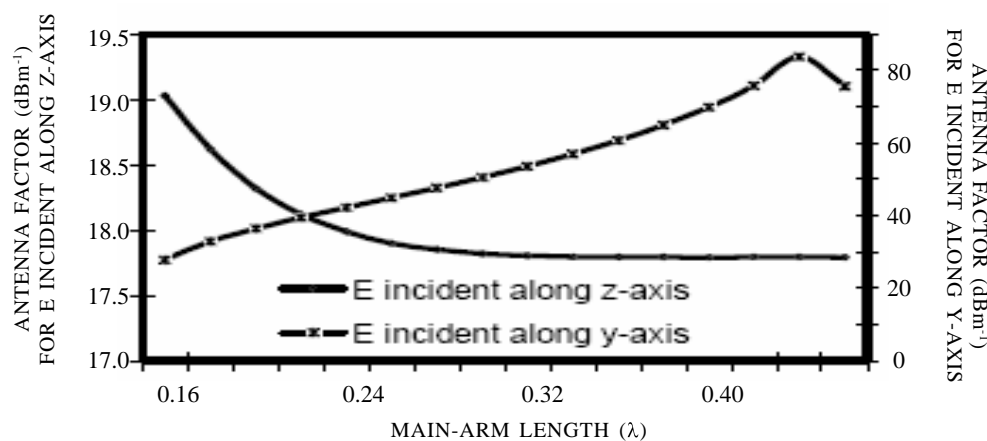


**Figure 12. Antenna factor (dBm⁻¹) versus length in wavelengths of I-shaped antenna.**

- The plot of antenna factor versus wavelength in Fig. 11 shows that the isolation for I-shaped antenna is better than 21.3 dBm⁻¹.

- The cross-polarisation isolation for C-shaped antenna (Fig. 12) is better than 0.22 dBm⁻¹.

  For a good receiver, the cross-polarisation pick-up of the antenna is expected to be minimum. Hence, the greater the value of cross polarisation isolation, the better is the performance of the antenna as sensor. From the study of different loaded antennas, it is seen that the cross-polarisation isolation of a T-shaped antenna is maximum i.e., the T-shaped resonant antenna is found as a better sensor compared to other loaded antennas/sensors.

  Also the correctness of the theory for the loaded sensor has been proved from the well-matching of the theoretical results to available experimental data (Fig. 13).
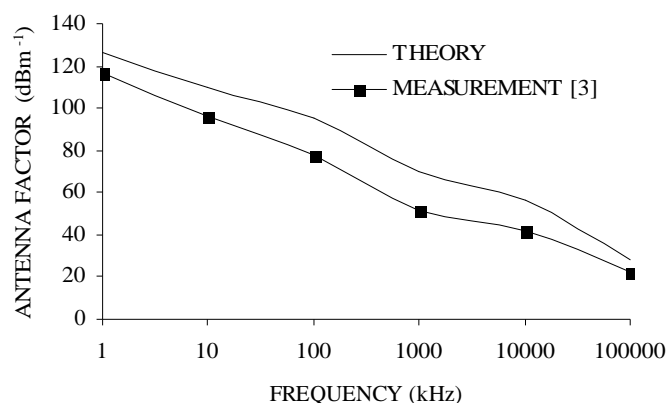


**Figure 13. Antenna factor versus frequency plot of a broadband dipole.**

# 5. CONCLUSION

It can be concluded that the height of the sensors can be appreciably reduced by the introduction of the load arms without making any major compromise in the performance in terms of cross-polarisation isolation.

## ACKNOWLEDGEMENT

## REFERENCES

1. Paul, C.R. Introduction to electromagnetic compatibility. New York, 1992.

2. Ted, L. Simpson. The theory of top-loaded antennas: Integral equations for the currents. *IEEE Trans. Antennas Propag.*, 1971, **AP-19**(2), 186-90.

3. Wang, K. & Nelson, R. Numerical simulation of the antenna factor of broad-band dipole antenna. *In* IEEE International Symposium on EMC, **1**, 2001, pp. 616-19.

4. Balanis, C.A. Antenna theory: Analysis and design, Ed. 2. John Wiley & Sons Inc, Singapore.

5. Ghosh, S.; Chakraborty, A. & Sanyal, S. Estimation of antenna factor of wire antenna as EMI sensor. *J. Electromag. Waves Appl.*, 2002, **16**(1), 79-91.

6. Ghosh, S.; Chakrabarty A. & Sanyal, S. Loaded wire antenna as EMI sensor. *In* Progress in Electromagnetics Research, PIER-54, 2005. pp. 19-36.

7. Ghosh, Saswati; Chakrabarty, Ajay & Sanyal, Subrata. Estimation of complex antenna factor of loaded wire antennas as EMI sensors. *In* Asia-Pacific Microwave Conference (APMC-04), 15-18 December 2004, New Delhi.

8. Kolundzija, B.M.; Ognjanovic, J.S. & Sarkar, T.K. WIPL-D: Electromagnetic Modelling of Composite Metallic and Dielectric Structures-Software and User's Manual, 1-332, Artech House.

9. Balanis, C.A. Advanced engineering electro-magnetics. John Wiley & Sons Inc., 1989, pp. 282-84.

10. Harrington, R.F. Field computation by moment methods. R.E. Krieger Publishing Co, Malabar, Florida. pp. 2-81.

## Contributors

**Dr (Ms) Saswati Ghosh** received her MSc (Radio Physics and Electronics) and MTech (Microwaves) from the Burdwan University, West Bengal, in 1995 and 1997 respectively and PhD from IIT Kharagpur in August 2004. Her research interests include: Effects of EMI/ESD on spacecraft bodies, EMI/EMC measurements, and EMI sensors.

**Prof Ajay Chakrabarty** received his MTech and PhD both from the IIT Kharagpur in 1977 and 1982 respectively. He joined the Radar Centre of Indian Institute of Technology Kharagpur in 1972. Currently, he is working at IIT Kharagpur in the Dept of Electronics and Electrical & Communication Engineering. His interests include: Array antenna design, antenna feeds, numerical modelling of waveguide junctions, and EMI/EMC measurements.